J. Opt. A: Pure Appl. Opt. **11** (2009) 114030 (6pp) doi:10.1088/1464-4258/11/11/114030

Nonlinear plasmonics with gold nanoparticle antennas

Stefano Palomba, Matthias Danckwerts and Lukas Novotny

Institute of Optics, University of Rochester, Rochester, NY 14627, USA[1]

Received 13 March 2009, accepted for publication 2 July 2009
Published 17 September 2009
Online at stacks.iop.org/JOptA/11/114030

Abstract
We investigate the nonlinear optical properties of gold nanoparticle pairs. Two excitation beams of frequencies ω_1 and ω_2 are used to induce nonlinear polarizations at the junction of a particle dimer. Nonlinearities of the second and third order can be controllably induced as a function of the dimer geometry, leading predominantly to second-harmonic generation (SHG), sum frequency generation (SFG) and four-wave mixing (4WM). Due to their center symmetry, dimers with identical particle diameters give rise to a very weak second-order response, without affecting the third-order response. Therefore, a sharp probe functionalized with a symmetric metal dimer acts as a nanoscale photon source emitting narrow-band photons of frequency $2\omega_1 - \omega_2$. We demonstrate that this source can be employed as a near-field optical probe for high-resolution fluorescence imaging.

Keywords: nonlinear plasmonics, four-wave mixing, second-harmonic generation, sum-frequency generation, near-field optics, nano-optics, plasmonics, near-field optical imaging

(Some figures in this article are in colour only in the electronic version)

1. Introduction

The interaction between an external electromagnetic field and a metal nanoparticle induces coherent oscillations of electrons and gives rise to a unique optical response associated with localized surface plasmon resonances (LSPR). These resonances can be tailored by the geometrical shape and the metal properties [1].

Metal nanostructures are also attractive from a perspective of photostability and chemical inertness. They find application in biophysical applications [2], labeling [3], particle tracking [4] and optical antennas [5]. When prepared as very small clusters they become highly fluorescent, water-soluble and do not suffer from photobleaching and photoblinking, which commonly affects dyes and semiconductor quantum dots [6]. Gold nanoparticles are also considered to be efficient nonlinear nanostructures due to their intrinsic nonlinearities [7–10]. It has been demonstrated that gold nanostructures generate a broad spectrum of two-photon excited luminescence spanning from the visible to the infrared [9], which is strongly influenced by the particle plasmon resonance [11].

[1] http://www.nano-optics.org.

Because of their inversion symmetry, the second-order nonlinear response of individual spherical gold nanoparticles is negligible. Nevertheless, weak second-harmonic generation (SHG) can still be observed due to small deviations from the perfectly spherical shape, due to surface defects, and due to higher-order multipole interactions between light and matter [12, 8]. Point symmetry does not affect the third-order nonlinear response of metal nanostructures and hence we can expect a higher yield of third-harmonic generation (THG) [13, 7] and four-wave mixing (4WM) [10] compared to sum-frequency generation (SFG) and second-harmonic generation (SHG) [8].

The interaction between two nanoparticles has been the subject of various theoretical studies [14–17], and several experiments on the single-particle level have been carried out recently [10, 18, 19, 17]. Nanoparticle pairs exhibit a very intense field enhancement at their junction [19] and the localized field gives rise to a strong nonlinear response. We have recently demonstrated that the efficiency of four-wave mixing at a gold nanoparticle dimer is very distance-sensitive; the 4WM intensity increases by four orders of magnitude within the last two nanometers of touching contact [10].

In this paper we investigate nonlinear frequency mixing at the junction of gold nanoparticle pairs and study the

geometrical symmetry dependence. The nonlinear response at the nanoparticle junction defines a highly localized, coherent and tunable photon source. We show that the 4WM intensity can be efficiently modulated and constitutes a possible building block for future plasmonic integrated devices. We demonstrate that the 4WM photon source can be used as a local excitation source for high-resolution near-field optical fluorescence imaging.

2. Experimental details

As illustrated in figure 1 we attach a gold nanoparticle dimer to the end of a pointed optical pipette. The latter are produced by a micropipette puller, cleaned in an oxygen plasma and then functionalized with (3-aminopropyl)trimethoxysilane (APTMES) at ∼90°. The functionalized pipettes are carefully attached to a quartz tuning fork and then positioned close to a sample surface with isolated gold nanoparticles by the use of shear-force control [20]. The gold nanoparticle sample consists of a mixture of ∼100 nm and ∼60 nm gold colloids spin-cast onto a Nanostrip cleaned coverglass slide. Some of the particles form symmetrical dimers (equal particle sizes) and others form asymmetrical dimers (unequal particle sizes) on the surface. The APTMES-treated pipette is then used as a shear-force probe to acquire topographic images of the sample and to identify isolated dimers. Once a dimer has been selected the probe is positioned over it and then approached to make chemical contact. This causes the dimer to be picked up by the probe. Subsequently, the resulting dimer probe is characterized under a scanning electron microscope (SEM). A representative image is shown in the inset of figure 1. The dimer probes produced by the outlined procedure consist of particle pairs that are predominantly aligned transverse to the axis of the pipette, thereby allowing the localized fields in the junction to directly interact with the sample surface. This arrangement is different from our previous work reported in [10] where the dimers were aligned along the tip axis.

In our experiments, the nanoparticle dimer antenna is excited (cf figure 1) by two incident laser beams of frequencies ω_1 and ω_2, respectively. The third-order susceptibility $\chi^{(3)}$ of the irradiated dimer gives rise to a nonlinear polarization at frequency $\omega_{4WM} = 2\omega_1 - \omega_2$, whereas its second-order susceptibility $\chi^{(2)}$ gives rise to a nonlinear polarization at frequency $\omega_{SHG} = 2\omega_2$ and at frequency $\omega_{SFG} = \omega_1 + \omega_2$. The frequencies of other nonlinear responses are either outside our detection band (430–630 nm) or are too weak to be detected. The pump beam at frequency ω_1 also generates a broad photoluminescence continuum originating from interband transitions of d-band electrons into the conduction band and subsequent radiative recombination [9]. The two laser beams are generated by a Ti:sapphire laser providing pulses of duration ∼200 fs, average power of ∼10–90 μW, repetition rate of ∼76 MHz and tunable wavelength of $\lambda_1 = 740$–821 nm. This laser also pumps an optical parametric oscillator (OPO) providing pulses of the same duration, average power of the order of ∼0.5–1 mW and tunable wavelength of $\lambda_2 = 1078$–1170 nm. A delay line accurately sets the time between the pulses of the two exciting beams. The third-order nonlinearity associated with four-wave mixing can be generated only when the two exciting beams are perfectly overlapping in time and space. Therefore, the 4WM signal generated at the nanoparticle junction can be switched 'ON' and 'OFF' very rapidly as a function of the time delay between the incident laser pulses.

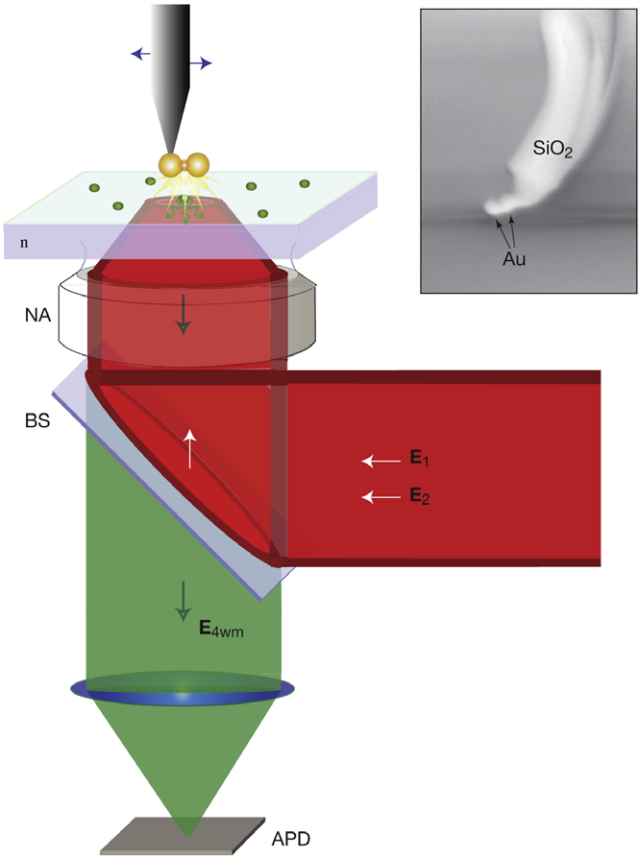

Figure 1. Illustration of the experimental set-up. A gold nanoparticle dimer attached to a sharply pointed optical fiber serves as a nonlinear photon source. The nanoparticle dimer is excited by two incident laser beams of frequencies ω_1 and ω_2, giving rise to four-wave mixing (4WM) at a frequency $\omega_{4WM} = 2\omega_1 - \omega_2$ generated at the nanoparticle junction. This localized source of radiation is used as a fluorescence excitation source for the sample placed underneath. A near-field fluorescence image is generated by raster scanning the sample and detecting pixel by pixel the fluorescence counts with a single-photon detector. Inset: electron micrograph of a nanoparticle dimer probe.

3. Results

The exciting lasers are tightly focused Gaussian beams (HG_{00}) incident along the surface normal of the sample surface. Because of the high numerical aperture the electric field in the focal plane exhibits significant longitudinal components, i.e. field components in the direction of propagation [21]. These longitudinal fields have been probed before by optical antennas made of a simple metal tip [22, 23]. The tip was raster-scanned through the focal plane and the emitted radiation due to linear scattering or SHG was recorded pixel

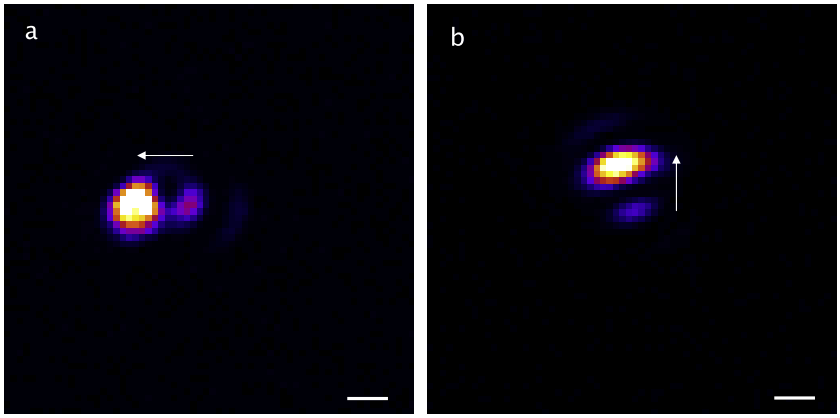

Figure 2. Polarization-dependent four-wave mixing (4WM) images of the laser focus. A vertical particle dimer antenna is raster-scanned through the two focused and overlapping stationary laser beams of frequency ω_1 and ω_2 and the intensity at frequency $2\omega_1 - \omega_2$ is recorded as a function of scan coordinates. The arrows in the figure represent the direction of polarization. The images represent the characteristic two lobes of the longitudinal incident field.

by pixel. Because of the large polarizability along the tip axis, the images resulting for a tightly focused Gaussian beam exhibit a characteristic two-lobe pattern [8]. These two lobes are oriented along the direction of the incident polarization. We performed similar experiments with a vertically oriented particle dimer antenna and recording the 4WM signal as this antenna was raster-scanned through the beam focus. In agreement with previous studies we observe the characteristic two lobes oriented in the direction of the incident polarization. The slight asymmetry in the images shown in figure 2 is due to a slight tilt of the particle dimer relative to the normal of the sample surface.

We next investigated the spectrum of the emitted photons from the junction of a dimer made of two unequal particle sizes as a function of excitation frequencies ω_1 and ω_2. The wavelengths were tuned from $\lambda_1 = 740$ and $\lambda_2 = 1078$ nm to $\lambda_1 = 821$ and $\lambda_2 = 1170$ nm. Full spectra of the emitted radiation were detected with a spectrometer in the wavelength range (430–630 nm) and are shown in figure 3. The geometrical asymmetry of the dimer defines a non-centrosymmetric system with substantial second-order nonlinear response. The spectra clearly show the peaks of 4WM ($\omega_{4WM} = 2\omega_1 - \omega_2$), SHG ($\omega_{SHG} = 2\omega_1$) and SFG ($\omega_{SFG} = \omega_1 + \omega_2$). Interestingly, as the excitation frequencies are tuned to the blue the intensity of the 4WM peak increases relative to the SHG and SFG peaks. Furthermore, at the same time the two-photon excited luminescence background decreases in strength. The slight intensity variations in figure 3 are mostly due to the particle dimer drifting out of laser focus.

Once the asymmetrical dimer is replaced by a dimer made of nanoparticles of equal size we observe a drastic reduction of the second-order nonlinear response (cf figure 4). The recorded spectrum exhibits only a single peak associated with 4WM at the particle junction and constitutes an ideal narrow-band excitation source for near-field optical imaging.

The third-order nonlinear response of gold nanoparticles is dominated by an ultrafast response (∼200 fs) due to interband electric-dipole transitions [24], comparable in time to the duration of the pump pulse. Therefore, it opens the door

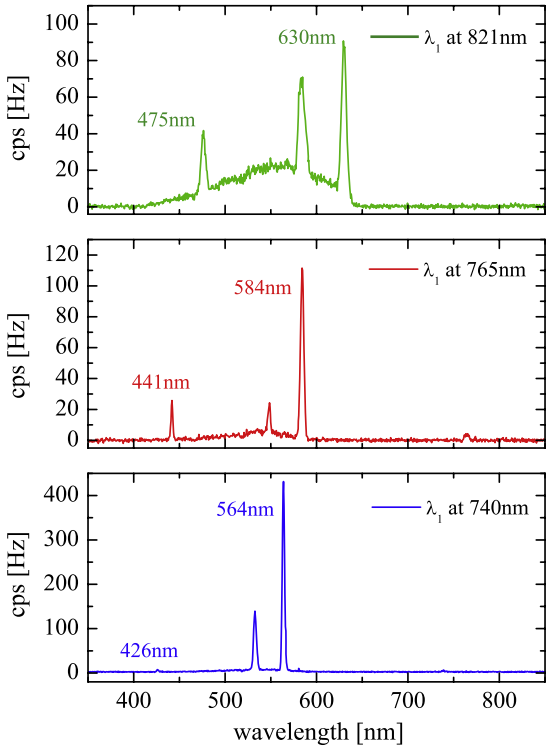

Figure 3. Spectra of photons emitted from an asymmetrical particle dimer as a function of excitation frequencies. The wavelengths are tuned from ($\lambda_1 = 821$ nm, $\lambda_2 = 1170$ nm) to ($\lambda_1 = 740$ nm, $\lambda_2 = 1078$ nm). The three peaks correspond to SHG, SFG and 4WM. The two-photon excited luminescence background becomes weaker as the excitation wavelengths are tuned to the blue.

for ultrafast modulation which, in the case of 4WM, can be accomplished by controlling the relative time delay between the two laser pulses. Another possibility, though slower, is to control the gap width between the two nanoparticles forming a dimer since it has been demonstrated that the 4WM intensity varies by four orders of magnitude within two nanometers of touching contact [10]. To demonstrate signal modulation by

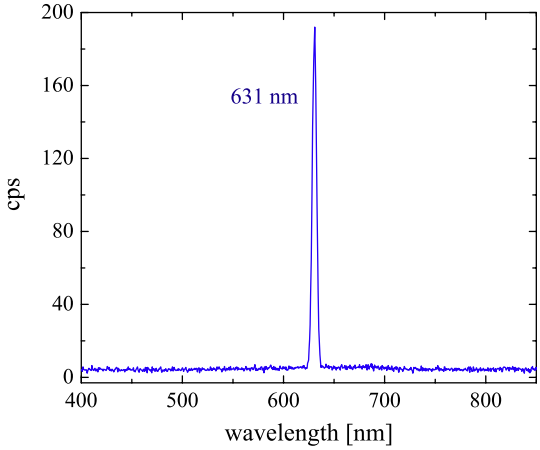

Figure 4. Spectrum of photons emitted from a symmetrical particle dimer, which is excited by laser beams of wavelengths $\lambda_1 = 821$ nm and $\lambda_2 = 1170$ nm, respectively. Due to the point symmetry the second-order nonlinear response is strongly suppressed and only the 4WM peak is observed.

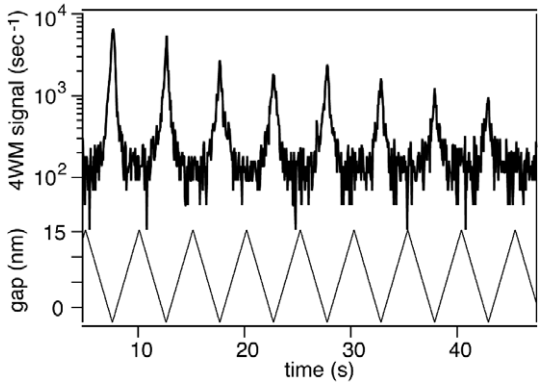

Figure 5. Modulation of the 4WM signal by varying the separation between a dimer made of two 80 nm gold nanoparticles. One of the particles is attached to a scanning probe tip whereas the other particle is immobilized on a MPTES-functionalized glass surface.

control of the gap width we immobilize one of the two 80 nm gold nanoparticles on a clean glass surface functionalized with (3-mercaptopropyl)trimethoxysilane (MPTMS) and attach the other particle to the tip of a pointed optical fiber. By use of shear-force feedback control [25] we bring the two gold nanoparticles close to each other and apply a 200 mHz triangular waveform to modulate the gap between the two particles. The 4WM signal is then recorded at the same time and a resulting time trace is shown in figure 5. The photon count rate is shown on a logarithmic scale in order to visualize the full scale of the signal modulation. Initially, the intensity at $\omega_{4WM} = 2\omega_1 - \omega_2$ is modulated by two orders of magnitude. This range can be increased by allowing the two particles to come even closer, but such short distances are difficult to control in a dynamic mode. The decrease in intensity of the 4WM signal shown in figure 5 is due to drift of the piezoelectric actuator used in the experiments. This drift can be eliminated by operating the modulation scheme with feedback control [26].

After having characterized the nonlinear and spectral properties of symmetric and asymmetric particle dimer antennas we exploit these localized light sources for high-resolution near-field optical imaging. For this purpose, a symmetric particle dimer is attached to the end of a pointed micropipette such that the joint axis of the particle dimer is nearly parallel to the sample surface. This configuration ensures that the localized 4WM source at the particle junction can be brought close to the sample surface. As a test sample we use a glass substrate with monodispersed red fluorescent microspheres (FluoSpheres, invitrogen). The absorption spectrum of the microspheres (∼40 nm in diameter) has a maximum at ∼660 nm. The corresponding fluorescence spectrum peaks at ∼680 nm. The optical antenna, made of two 80 nm gold particles, is excited by ∼200 fs laser pulses of wavelength $\lambda_1 = 821$ nm and $\lambda_2 = 1170$ nm, respectively, and produces emission at the four-wave mixing frequency $\lambda_{4WM} = 630$ nm (cf figure 5), which is close to the absorption peak of the microspheres. The dimer antennas are positioned in the stationary laser foci such that the emitted 4WM intensity is maximized. Subsequently, the sample with the fluorescent microspheres is raster-scanned underneath the optical antenna while detecting the fluorescence in the wavelength range of (694–738) nm, defined by optical bandpass filters. Simultaneously, we record the topography of the sample by monitoring the vertical motion of the particle dimer antenna during shear-force feedback.

As shown in figures 6(a)–(d), we clearly observe a fluorescence signal every time the particle dimer is positioned over a fluorescent microsphere. Each microsphere gives rise to a double-lobe pattern in the topographic image, which reflects the geometrical shape of the dimer. In other words, because of its smaller size each microsphere acts as a probe for the optical antenna and thereby traces out its particular shape. Each topographic feature has a corresponding optical feature, which demonstrates that the 4WM signal generated at the particle junction can be employed as an effective fluorescence excitation source. To prove that the observed fluorescence originates from 4WM excitation we repeat the same measurements with a delay between the excitation pulses. This delay no longer allows the 4WM signal to be generated and hence there should be no excitation of the fluorescent particles. This is indeed what is observed in figures 6(e) and (f). The residual background in the optical image originates mainly from two-photon excited luminescence emitted by the dimer antenna. This luminescence passes through the fluorescence bandpass filters and cannot be separated from the microsphere fluorescence. Time-correlated photon counting will make it possible to discriminate the microsphere fluorescence from the metal's luminescence background because the excited-state lifetimes of the two processes are very different. The characteristic lifetime of two-photon excited luminescence is shorter than 10 ps [9] whereas typical fluorescence lifetimes of molecules are at least ten times longer, even in the presence of the optical antenna [27]. Therefore, we expect that the signal-to-noise ratio of our near-field imaging method can be considerably improved.

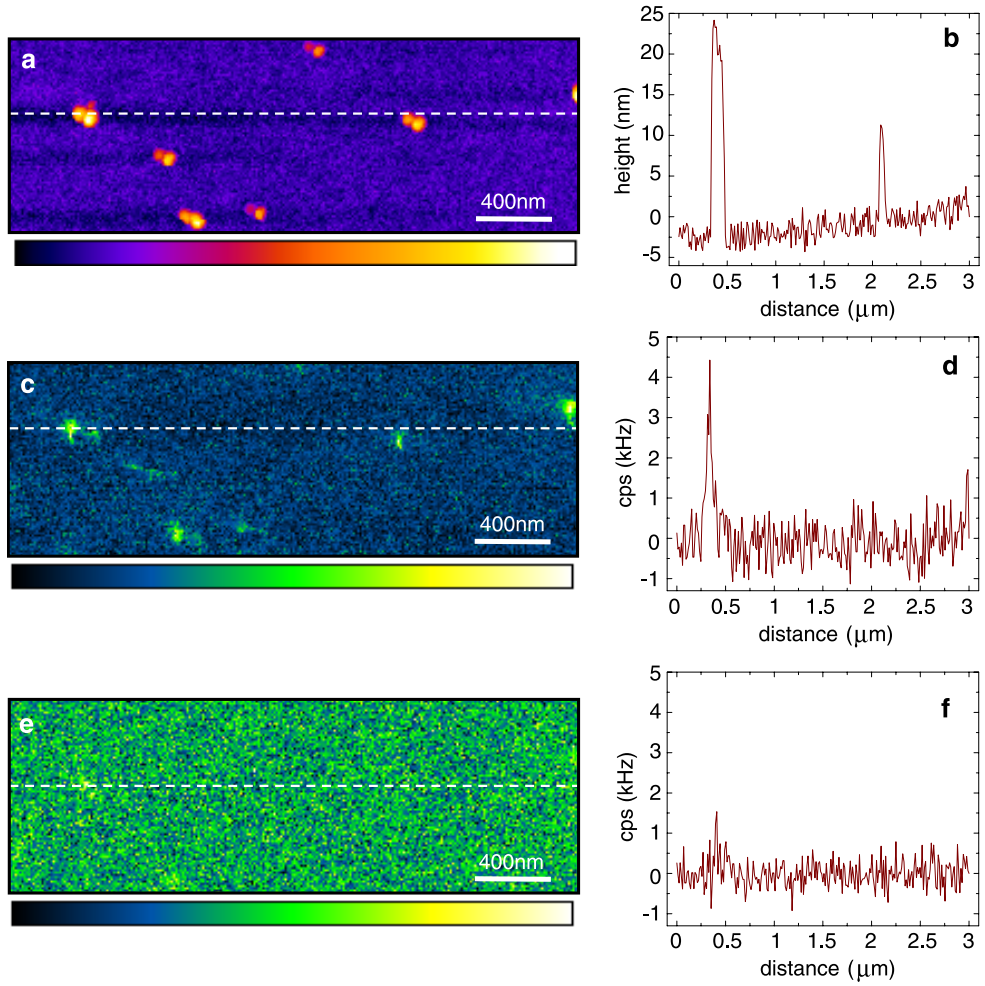

Figure 6. Near-field fluorescence imaging with a localized 4WM photon source. (a) Topographic image of ∼40 nm microspheres. The double-lobed features reflect the geometrical shape of the particle dimer antenna. (c) Simultaneous near-field fluorescence image recorded by integrating the emitted fluorescence photons in the wavelength range (694–738) nm. (e) Near-field fluorescence image recorded by turning off the 4WM generation by introducing a time delay between the incident laser pulses at frequencies ω_1 and ω_2. (b), (d), (f) Linecuts evaluated along the lines indicated in (a), (c) and (e), respectively.

4. Conclusions

We have demonstrated that the nonlinear response at a gold nanoparticle junction defines a localized, tunable and narrow-band photon source. This photon source can be employed for high-resolution fluorescence imaging. The relative strength of second-order and third-order nonlinearities can be influenced by the symmetry of the particle dimer. For a symmetric dimer, made of two nanoparticles of equal size, the second-order response is negligible and we observe basically no SHG and SFG. The only nonlinear response that survives in the visible frequency range is the 4WM signal. Modulation of the junction by a few nanometers gives rise to a large modulation of the 4WM intensity, a property that can be exploited in optoelectronic devices. Because the wavelength of the 4WM signal can be tuned over a wide spectral range this signal is also ideally suited for local extinction measurements. We estimate that it should be possible to reach single-molecule sensitivity with this interaction scheme.

Acknowledgments

We thank Christiane Höppener and Palash Bharadwaj for help with sample preparation. This work was supported by the National Science Foundation (grant ECCS-0651079) and the US Department of Energy (grant DE-FG02-01ER15204).

References

[1] Kreibig U, Bour G, Hilger A and Gartz M 1999 Optical properties of cluster-matter: influences of interfaces *Phys. Status Solidi* a **175** 351–66
[2] Stanley J K *et al* 2007 A cellular trojan horse for delivery of therapeutic nanoparticles into tumors *Nano Lett.* **7** 3759–65
[3] Seydack M 2005 Nanoparticles labels in immunosensing using optical detection methods *Biophys. J.* **20** 2454–69
[4] Brunner C, Vogel V, Jacobsen V, Stoller P and Sandoghdar V 2006 Interferometric optical detection and tracking of very small gold nanoparticles at a water–glass interface *Opt. Express* **14** 405–14
[5] Bharadwaj P, Anger P and Novotny L 2007 Nanoplasmonic enhancement of single-molecule fluorescence *Nanotechnology* **18** 044017

[6] Zheng J, Zhang C and Dickson R M 2004 Highly fluorescent, water-soluble, size-tunable gold quantum dots *Phys. Rev. Lett.* **93** 077402
[7] Lippitz M, van Dijk M A and Orrit M 2005 Third-harmonic generation from single gold nanoparticles *Nano Lett.* **5** 799
[8] Bouhelier A, Beversluis M, Hartschuh A and Novotny L 2003 Near-field second-harmonic generation induced by local field enhancement *Phys. Rev. Lett.* **90** 13903
[9] Beversluis M R, Bouhelier A and Novotny L 2003 Continuum generation from single gold nanostructures through near-field mediated intraband transitions *Phys. Rev.* B **68** 115433
[10] Danckwerts M and Novotny L 2007 Optical frequency mixing at coupled gold nanoparticles *Phys. Rev. Lett.* **98** 026104
[11] Bouhelier A and Wiederrecht G P 2005 Excitation of broadband surface plasmon polaritons: plasmonic continuum spectroscopy *Phys. Rev.* B **71** 195406–13
[12] Boyd R W 2002 *Nonlinear Optics* 2nd edn (San Diego, CA: Academic)
[13] Sarger L, Barille R, Vacher P, Canioni L, Rivet S and Voisin P 2001 Imaging of Ca^{2+} intracellular dynamics with a third-harmonic generation microscope *Opt. Lett.* **26** 515–7
[14] Ghosh S K and Pal T 2007 Interparticle coupling effect on the surface plasmon resonance of gold nanoparticles: from theory to applications *Chem. Rev.* **107** 4797–862
[15] Wenzel M T, Olk P, Renger J and Eng L M 2008 Distance dependent spectral tuning of two coupled metal nanoparticles *Nano Lett.* **8** 1174–8
[16] Nordlander P, Willingham B and Brandl D W 2008 Plasmon hybridization in nanorod dimers *Appl. Phys.* B **93** 209–16
[17] Huang W, Prashant K J and El-Sayed M A 2007 On the universal scaling behavior of the distance decay of plasmon coupling in metal nanoparticle pairs: a plasmon ruler equation *Nano Lett.* **7** 2080–8
[18] Lassiter J B, Aizpurua J, Hernandez L I, Brandl D W, Romero I, Lal S, Hafner J H, Nordlander P and Halas N J 2008 Close encounters between two nanoshells *Nano Lett.* **8** 1212–8
[19] Talley C E, Jackson J B, Oubre C, Grady N K, Hollars C W, Lane S M, Huser T R, Nordlander P and Halas N J 2005 Surface-enhanced raman scattering from individual Au nanoparticles and nanoparticle dimer substrates *Nano Lett.* **5** 1569–74
[20] Hoeppener C and Novotny L 2008 Antenna-based optical imaging of single Ca^{2+} transmembrane proteins in liquids *Nano Lett.* **8** 642–6
[21] Novotny L and Hecht B 2006 *Principles of Nano-Optics* (Cambridge: Cambridge University Press)
[22] Bouhelier A, Beversluis M and Novotny L 2003 Near-field scattering of longitudinal fields *Appl. Phys. Lett.* **82** 4596
[23] Bouhelier A, Beversluis M R and Novotny L 2003 Characterization of nanoplasmonic structures by locally excited photoluminescence *Appl. Phys. Lett.* **83** 5041–3
[24] Liao H B, Xiao R F, Fu J S, Wang H, Wong K S and Wong G K L 1998 Origin of third-order optical nonlinearity in Au:SiO_2 composite films on femtosecond and picosecond timescales *Opt. Lett.* **23** 388–90
[25] Karrai K and Grober R D 1995 Piezoelectric tip–sample distance control for near field optical microscopes *Appl. Phys. Lett.* **66** 1842–4
[26] Höppener C, Beams R and Novotny L 2009 Background suppression in near-field optical imaging *Nano Lett.* **9** 903–8
[27] Kühn S, Hakanson U, Rogobete L and Sandoghdar V 2006 Enhancement of single-molecule fluorescence using a gold nanoparticle as an optical nanoantenna *Phys. Rev. Lett.* **97** 017402